

Modification of jets travelling through a brick-like medium

Chiara Le Roux^a, José Guilherme Milhano^{b,c}, Korinna Zapp^a

^a*Dept. of Physics Lund University Slvegatan 14A S22362 Lund Sweden*

^b*LIP Av. Prof. Gama Pinto 2 P-1649-003 Lisboa Portugal*

^c*Departamento de Física Instituto Superior Técnico (IST) Universidade de Lisboa Av. Rovisco Paes 1 P-1049-001 Lisboa Portugal*

Abstract

It is a continued open question how there can be an azimuthal anisotropy of high p_\perp particles quantified by a sizable v_2 in p+Pb collisions when, at the same time, the nuclear modification factor R_{AA} is consistent with unity. We address this puzzle within the framework of the jet quenching model JEWEL. In the absence of reliable medium models for small collision systems we use the number of scatterings per parton times the squared Debye mass to characterise the strength of medium modifications. Working with a simple brick medium model we show that, for small systems and not too strong modifications, R_{AA} and v_2 approximately scale with this quantity. We find that a comparatively large number of scatterings is needed to generate measurable jet quenching. Our results indicate that the R_{AA} corresponding to the observed v_2 could fall within the experimental uncertainty. Thus, while there is currently no contradiction with the measurements, our results indicate that v_2 and R_{AA} go hand-in-hand. We also discuss departures from scaling, in particular due to sizable inelastic energy loss.

1. Introduction

In the field of relativistic heavy ion collisions, the idea that high energy partons traveling through a medium will lose energy due to successive interactions with the medium constituents has long been established from the theoretical point of view [1, 2] and subsequently confirmed experimentally [3, 4] via the measurement of nuclear modification factors, which compare the yields of high p_\perp particles in heavy ion collisions to that in pp collisions, where no medium was expected to be formed. These measurements were then repeated in small systems collisions such as d+Au and p+Pb and the absence of quenching was confirmed [5, 6, 7, 8, 9, 10, 11, 12]. Such results motivated the interpretation of this suppression as a signature of the presence of a quark gluon plasma (QGP) phase in the early stages of relativistic heavy ion collisions.

As a means to investigate this newly discovered, short lived phase of matter, several other observables were proposed. One of them is the azimuthal momentum anisotropy, which is commonly characterised via the flow coefficients v_n appearing in the Fourier decomposition of the particle distribution

$$\frac{dN}{d\phi} = \frac{1}{2} \left(1 + 2 \sum_n v_n \cos(2(\phi - \Psi_n)) \right). \quad (1)$$

Here, Ψ_n is the azimuthal angle of the n^{th} symmetry plane. Since the overlap region of two colliding nuclei has a strong elliptical deformation, the corresponding elliptical term in the momentum distribution, v_2 , is the most prominent one in heavy ion collisions. For $n = 2$, Ψ_2 is the orientation of short axis of the overlap region. Therefore, if $v_2 = 0$ (and

thus all the v_n for $n > 0$ also are), that means that this distribution is completely isotropic and, as it acquires an ellipsoidal shape, one starts observing a non-zero v_2 .

Several experiments have measured the flow coefficients and found a non-zero v_2 in relativistic heavy ion collisions [13, 14, 15, 16, 17]. In these collisions a non-vanishing v_2 of low transverse momentum particles is a consequence of the collective flow of the system. Because the pressure gradient driving the expansion is larger along the short axis of the overlap region than along the long axis the particles are pushed out preferentially along the short axis. At high p_\perp , v_2 is generated via the path length dependence of the energy loss suffered by the hard particle. It is thus also a consequence of the geometry of the system, but is not related to collective flow.

Surprisingly, sizable flow coefficients, in particular v_2 , were also observed in small systems [18, 19]. These systems are believed to be too short lived to develop collective flow, but it has been shown in kinetic theory that even with a low number of scatterings per particle a sizable v_2 can be generated via the so-called escape mechanism [20, 21, 22, 23, 24]. On the other hand, an explanation in terms of a hydrodynamic evolution of the system has also been put forward [25] (and criticised in [26]).

While viable explanations thus exist for the observation of non-vanishing v_2 of soft particles in small collision systems, the same is not true for the v_2 of high p_\perp particles found in such systems [27, 28, 29]. According to our current understanding that would have to be generated by anisotropic energy loss, but the absence of jet quenching contradicts such an interpretation. However, the question really remains a quantitative one, namely whether it is

possible that a small amount of energy loss could generate a measurable high $p_{\perp} v_2$ while not leading to a measurable R_{AA} of hard particles or jets.

The present work aims to address precisely that question. To model the energy loss of hard partons, the JEWEL event generator is used. However, usually one must make assumptions of what a medium looks like and how it should expand, which, in turn, adds uncertainties about the assumptions in the specific the medium model used. In order to reduce the dependence on the medium model, we take a different approach and look specifically into how many jet-medium interactions (or actually what is the magnitude of the average number of interactions per jet particle times the Debye mass of the medium, $\langle n_{\text{int}} \rangle \cdot (DM)^2$, as will be discussed in the later sections) one needs in order to see the aforementioned observables. Therefore, we perform this study using a simplified medium model and then, knowing the $\langle n_{\text{int}} \rangle \cdot (DM)^2$ needed to get effects of a given magnitude, one can look into more realistic media.

2. JEWEL Monte Carlo Model

The Monte Carlo model JEWEL [30] simulates the QCD evolution of highly energetic partons produced in hard scattering processes in the presence of a background medium. It is based on PYTHIA 6.4 [31], which provides the hard scattering matrix elements, initial state parton shower and hadronisation. JEWEL has a virtuality ordered final state parton shower that is similar but not identical to the virtuality ordered parton shower in Pythia 6. In vacuum this is an ordinary parton shower with the somewhat special feature that recoils from splittings are handled locally and in such a way that the algorithm never goes back to modify the kinematics of an earlier splitting. In the presence of a coloured medium scattering off medium constituents can occur between the splittings generated by the parton shower. The scatterings are described by pQCD t -channel matrix elements regularised by a screening mass. If such a scattering is harder than the current parton shower scale it can reset the parton shower and re-start at the scale of the scattering. In this way medium induced bremsstrahlung is effectively included and it is ensured that elastic and inelastic scattering occur with the leading log correct relative rates. The Landau-Pomeranchuk-Migdal effect [32, 33] is included by allowing subsequent scatterings to act coherently if they fall within the formation time of the first splitting of a re-started parton shower. The momentum transfers are then added vectorially and the emission gets re-weighted with the inverse of the number of coherent momentum transfers. This procedure was shown to reproduce the BDMPS result in the eikonal limit [34]. Finally, re-starting the parton shower is only allowed when the first emission from the new shower has a shorter formation time than the current emission from the old shower. The medium partons recoiling from an interaction with a hard parton can be kept in the event to provide a simple

model of medium response. The parton shower partons and where applicable the recoils are hadronised with the PYTHIA string hadronisation.

JEWEL is largely agnostic about the background medium and it is therefore possible to interface different medium models. However, it only simulates jets and medium response, but not the evolution of the bulk medium. Therefore, the events contain only particles that belong to the hard scattering and the parton showers or that have interacted with such a parton.

3. The small systems set-up

To address the puzzle of v_2 and R_{AA} in small systems we have used JEWEL with a *brick*-like medium. This medium model consists of a collection of gluons distributed in an ellipsoidal region of space over which the temperature and density are uniform. The geometry of this region is defined by two input parameters: the length of the long axis of that ellipse (or sphere in case the eccentricity is zero) and its eccentricity. The density and temperature can also be specified by input parameters. The Debye mass, which regularises the scattering cross section and thus controls the hardness of the interactions is related to the temperature in the default JEWEL setup. We here decouple it from the temperature and make it a free parameter to be able to disentangle dependencies.

With this medium set up, we produce events for each set of medium parameters. All of the events (in medium or vacuum) used for the results in the upcoming sections are di-jet events at 5.02 TeV created with p_{\perp} within 50 and 500 GeV within a pseudo rapidity range of 3.1. In order to remove path length dependence (apart from the natural one coming from the geometry of the medium), we always generate the di-jets at the center of the brick. Then, we allow them to evolve and interact with the medium while counting the number of jet-medium interactions. In order to remove any biases related to the jet fragmentation pattern, we calculate the observables of interest as a function of the average number of interactions at a given density. In other words, the number of interactions is tuned by changing the density while keeping the temperature and the system size and geometry fixed.

The two observables studied in the present work were R_{AA} and v_2 . To compute them, we take all the final state hadrons with $p_{\perp} \leq 0.5$ GeV within a pseudo rapidity range of 2.8. Then, for R_{AA} , we reconstruct the jets using the anti- k_{\perp} algorithm with a radius of 0.4. We then obtain the p_{\perp} distributions of the reconstructed jets and, to quantify this and plot it against the number of jet-medium interactions, we integrate the p_{\perp} spectra between 100 and 400 GeV and, finally, we take the ratio of the medium result to the vacuum one.

As for the v_2 , the default way to obtain it in small systems would be via correlations with soft particles forming a background to the ones coming from the hard scattering. This is done because the event plane in those sys-

tems is not well defined. However, the soft background is not available in JEWEL. We thus make use of equation 1 keeping in mind that, since the geometry of the brick is manually defined, then the symmetry plane is known, i.e., Ψ_2 is known. With that, and assuming all $v_{n>2} \approx 0$, we fit equation 1 to the azimuthal angle distribution of all hadrons with $p_\perp \geq 2$ GeV and extract v_2 as a parameter of the fit. This is done event by event and the v_2 for a given set of parameters is the average for all the events with that set.

4. Results

As aforementioned, in order to obtain R_{AA} and v_2 as a function of the average number of jet-medium interactions, the density is varied while keeping the other medium parameters fixed. This way, we obtain events with some distribution of number of interactions, shown in FIG. 1, with a pronounced peak at the average value.

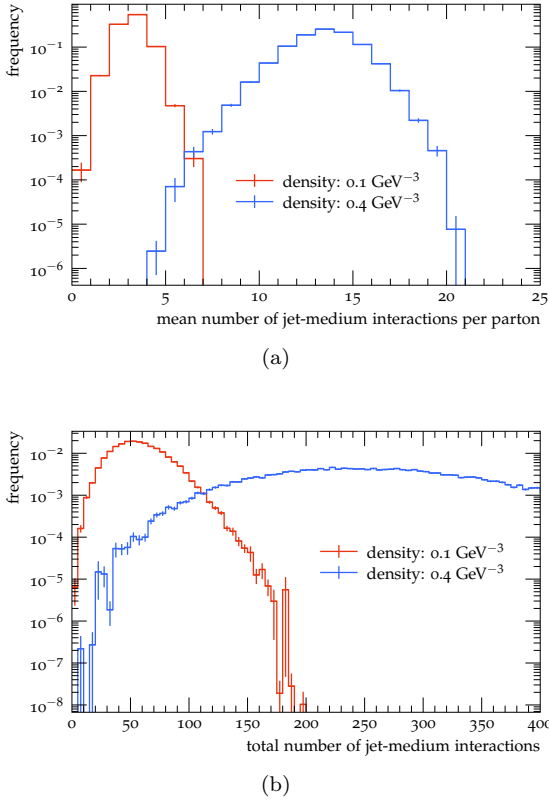


Figure 1: Distributions of mean number of interactions per parton (a) of total number of jet-medium interactions (b).

We thus proceed with studying the R_{AA} dependence with the number of interactions. However, instead of plotting the results as a function of the number of jet-medium interactions, we plot them against the average number of interactions per parton ($\langle n_{int} \rangle$) times the square of the Debye mass (DM), which is a proxy for the average momentum squared exchanged per parton between jet and

medium. This is done because the DM of the medium particles controls how hard the interactions are, which strongly affects the energy loss per interaction and, therefore, the R_{AA} .¹ Therefore, we calculate R_{AA} and v_2 as a function of $\langle n_{int} \rangle \cdot (\text{DM})^2$ for two different values of the DM, as seen in FIG. 2. The number of interactions per parton is calculated taking into account the entire (splitting) history of the partons. At the end of the partonic phase we find all partons present at that stage. We then follow each parton backwards through the evolution counting the number of scatterings. When a splitting is reached we continue with the mother parton. In this way all scatterings in the history of the parton are counted.

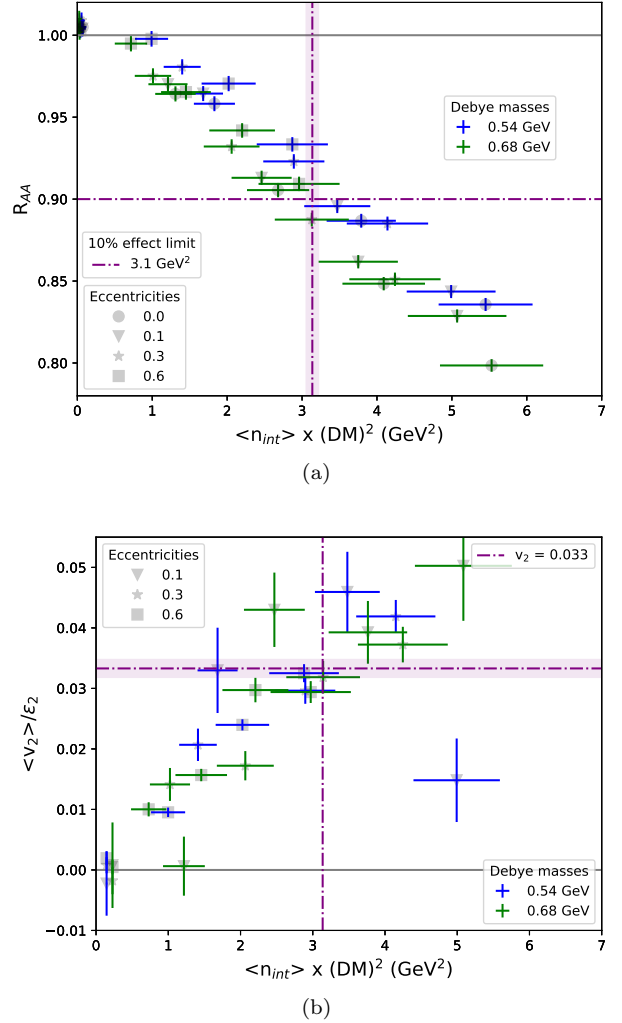


Figure 2: (a) R_{AA} and (b) v_2 results also as a function of $\langle n_{int} \rangle \cdot (\text{DM})^2$.

FIG. 2 shows that both R_{AA} and v_2 scale almost linearly with $\langle n_{int} \rangle \cdot (\text{DM})^2$. The dot dashed lines in FIG. 2(a) show the point at which the R_{AA} goes below 0.9,

¹In a single scattering the energy loss of the energetic parton scales approximately as $(\text{DM})^2$.

which is around the value of R_{AA} that can be safely measured. The lines show that this happens at $3.1(1) \text{ GeV}^2$, corresponding to 12 interactions per parton in the case of $DM=0.55 \text{ GeV}$ and around 8 interactions $DM=0.68 \text{ GeV}$. These numbers correspond to a total of around 100 to 150 jet-medium interactions.

On the other hand, FIG. 2(b) shows the result of v_2 divided by the eccentricity (ϵ_2) of the brick. This is done because v_2 is proportional to ϵ_2 and in this way one can determine how v_2 scales with the number of interactions for any medium eccentricity. In this case, the dot dashed lines show the value of v_2 at the same point where a 10% effect in R_{AA} was observed in FIG. 2(a). That is, for $\langle n_{\text{int}} \rangle \cdot (DM)^2 = 3.5 \text{ GeV}^2$, $v_2 / \epsilon_2 = 0.033(1)$, which corresponds to $v_2 = 0.0099(3)$ for an intermediate eccentricity of 0.3. The eccentricity is calculated from the position of the scatterings using $\epsilon_2 = \langle y^2 - x^2 \rangle / \langle x^2 + y^2 \rangle$.

It should be noted that, when computing v_2 in the way described in section 3, i.e. relative to the symmetry plane, it should be considered as an underestimate of the values obtained in experiments from two particle correlations. The latter is generically larger than the former, for instance because it responds differently to fluctuations. We thus don't see our results as a contradiction to the measurements. Nonetheless, these results indicate that, if the system has interacted enough to produce a v_2 of high p_\perp particles through path length dependent energy loss, then R_{AA} should show substantial suppression already.

We also verified the range of validity of this linear scaling with $\langle n_{\text{int}} \rangle \cdot (DM)^2$. For that, we plotted the R_{AA} as a function of brick radius for different points with the same $\langle n_{\text{int}} \rangle \cdot (DM)^2$, as shown in FIG. 3. It shows that, as the size of the medium increases, the same value of $\langle n_{\text{int}} \rangle \cdot (DM)^2$ produces more suppression when compared with the smaller medium. This is most pronounced for higher values of the Debye mass. In JEWEL the amount of medium induced radiation depends rather strongly on the Debye mass, because it is much easier for harder scatterings to initiate medium induced emissions. It is also easier for a scattering to induce an emission at later times, because then there is less competition from the parton shower of the initial hard scattering. This leads to an increase of medium induced emissions per scattering as a function of system size as seen in Fig. 3. Thus, when the inelastic interactions are turned off (i.e. there is only elastic scattering), this suppression is not as important. This indicates that the breaking of this scaling is largely due to a sizable contribution from inelastic interactions. This can also be seen in FIG. 3(b), where we show the difference in number of splittings between jets with the same generation parameters in vacuum and in medium for the corresponding points in 3(a). It is worth noting that, in the medium, angular ordering is not imposed between two splittings if an interaction has taken place between them. Therefore, even the points with only elastic interactions are expected to have more splitting than the jets in vacuum. As for the remaining difference, it is accounted for by

medium induced emissions. Therefore, the plots in FIG. 3(b) indicate that inelastic energy loss does not follow the scaling, and in small systems where the scaling approximately holds, energy loss is mainly driven by elastic interactions. Fig. 3 also shows that, while inelastic energy loss is an important factor for departures from scaling, there is an effect even in the absence of inelastic scattering. This is because, even for elastic scattering, the time at which a scattering occurs is not completely irrelevant (as assumed by the scaling). At early times the partons did not have time to radiate much yet and therefore the average parton energy is higher than at later times. A higher parton energy implies a smaller energy loss for the same momentum transfer and an early scattering thus leads to a somewhat smaller energy loss than a later one. Also, early scatterings contribute less to broadening, which transports energy out of the jet cone. This is so because a scattering of a parton early in the branching history tends to deflect the whole jet rather than individual constituents of the jet.

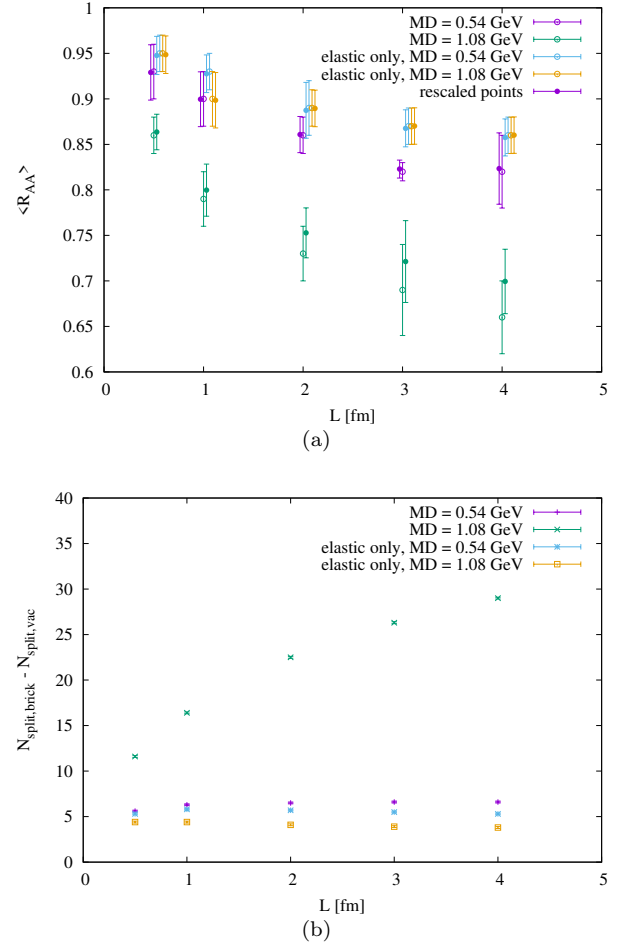


Figure 3: (a) R_{AA} as a function of brick radius for points with similar $\langle n_{\text{int}} \rangle \cdot (DM)^2$. Since the points have slightly different $\langle n_{\text{int}} \rangle \cdot (DM)^2$ we have rescaled R_{AA} to a common $\langle n_{\text{int}} \rangle \cdot (DM)^2 = 3.5 \text{ GeV}^2$ assuming a linear dependence of R_{AA} on $\langle n_{\text{int}} \rangle \cdot (DM)^2$. (b) Difference in number of splittings between the medium simulations and the corresponding vacuum corresponding to the points in (a).

Finally, we also generated events using a somewhat more realistic medium model, which accounts for longitudinal expansion and has a temperature profile. This is the simplistic medium model that comes with JEWEL [30]. We want to stress that this by no means a realistic model, and in particular it is expected to perform poorly for small systems [35]. The motivation for using it here is rather to have a model that is qualitatively different from the brick medium. We started by looking into OO events and saw that the R_{AA} suppression with $\langle n_{\text{int}} \rangle \cdot (DM)^2$ was much faster than with the brick. However, even at OO, the effective size of the medium was significantly larger than our 1 fm brick. Therefore, in light of the results in FIG. 3, we could not directly compare the two. We then moved to even smaller systems (HeHe and deuteron-deuteron) and the R_{AA} dependence with $\langle n_{\text{int}} \rangle \cdot (DM)^2$ became closer to that shown in FIG. 2, although the suppression is still significantly steeper, as shown in FIG. 4.

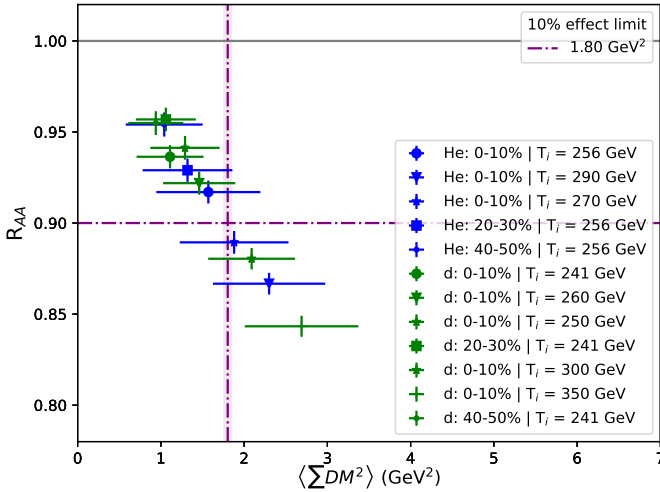


Figure 4: R_{AA} as a function of $\langle \sum DM^2 \rangle$ for the expanding medium, where $\langle \sum DM^2 \rangle$ stands for the average sum of DM^2 for each interaction per parton, i.e., it is the same as $\langle n_{\text{int}} \rangle \cdot (DM)^2$, which was used for the brick, but where the DM is allowed to vary.

However, this divergence from the result in FIG. 2(a) could be due to the fact that the medium model used was not tailored for application in small systems and may be faulty there. In particular it has a linear increase of the temperature until the initial proper time τ_i (after which longitudinal expansion leads to a decreasing temperature). The points shown here were generated with $\tau_i = \text{unit}[0.4] \text{ fm}$, which is a large fraction of the total size and lifetime of a small collision system. Most scatterings thus occur at relatively late times and Fig. 3 indicates that this is expected to lead to a stronger suppression. Nonetheless, FIG. 4 also shows a scaling of the R_{AA} with $\langle \sum DM^2 \rangle$, thus supporting the finding with the brick.

5. Conclusions

We have studied how the number of jet-medium interactions affects different jet quenching observables. The first important observation is that the result is largely dependent on the screening mass of the medium and, in fact, R_{AA} and v_2 scale approximately with $\langle n_{\text{int}} \rangle \cdot (DM)^2$. FIG. 2 shows how these observables depend on $\langle n_{\text{int}} \rangle \cdot (DM)^2$ and that at 3.1(1) GeV² a 10% effect is observed in R_{AA} . At the same point, and for the intermediate eccentricity studied ($\epsilon_2 = 0.3$), $v_2 = 0.0099(3)$. This value of $\langle n_{\text{int}} \rangle \cdot (DM)^2$ corresponds to between 8 and 12 interactions per parton in the range of Debye masses studied. This means that, in total, around 100 interactions between jet and medium particles are required to obtain an observable R_{AA} in small systems. But we have also studied the validity of this scaling behavior and 3(b) shows that it breaks down for larger systems sizes. It also shows that when the system size is small, the energy loss happens mainly through elastic scatterings. The reasons for departure from scaling are radiative energy loss, which does not follow the scaling and in JEWEL is more important at later times, and the fact that elastic scattering is more effective for jet quenching when it occurs at later times. Finally, we looked at a more realistic medium model and saw that the R_{AA} dependence with $\langle n_{\text{int}} \rangle \cdot (DM)^2$ observed in FIG. 2(a) did not hold, although it became closer to that when looked at a smaller system size. Therefore, this shows that there is a scaling behavior of the R_{AA} with the number of scatterings and the square of the Debye mass, but the size of the system plays a strong role in how this scaling looks like.

Acknowledgments

We would like to thank Alice Ohlson for enlightening discussions. This study is part of a project that has received funding from the European Research Council (ERC) under the European Union's Horizon 2020 research and innovation programme (Grant agreement No. 803183, collectiveQCD). JGM was partly supported by the European Research Council project ERC-2018-ADG-835105 YoctoLHC.

References

- [1] James Daniel Bjorken. Energy loss of energetic partons in quark - gluon plasma: Possible extinction of high $p(t)$ jets in hadron - hadron collisions. *FERMILAB-PUB*, 82, 1982.
- [2] R. Baier, Yu.L. Dokshitzer, A.H. Mueller, S. Peigné, and D. Schiff. Radiative energy loss of high energy quarks and gluons in a finite-volume quark-gluon plasma. *Nuclear Physics B*, 483(1):291–320, 1997.
- [3] K. Aamodt and et al. Suppression of charged particle production at large transverse momentum in central pbbp collisions at $\sqrt{s_{NN}}=2.76$ tev. *Physics Letters B*, 696(1):30–39, 2011.
- [4] C. Adler and et al. Centrality dependence of high- p_T hadron suppression in Au + Au collisions at $\sqrt{s_{NN}} = 130$ GeV. *Phys. Rev. Lett.*, 89:202301, Oct 2002.
- [5] J. Adams and et al. Evidence from $d + \text{Au}$ measurements for final-state suppression of high- p_T hadrons in Au + Au collisions at rhic. *Phys. Rev. Lett.*, 91:072304, Aug 2003.

- [6] B. Abelev and et al. Transverse momentum distribution and nuclear modification factor of charged particles in p +Pb collisions at $\sqrt{s_{NN}}=5.02$ TeV. *Phys. Rev. Lett.*, 110:082302, Feb 2013.
- [7] Jaroslav Adam et al. Measurement of charged jet production cross sections and nuclear modification in p -pb collisions at $\sqrt{s_{NN}} = 5.02$ tev. *Phys. Lett. B*, 749:68–81, 2015.
- [8] Vardan Khachatryan et al. Transverse momentum spectra of inclusive b jets in pPb collisions at $\sqrt{s_{NN}} = 5.02$ TeV. *Phys. Lett. B*, 754:59, 2016.
- [9] Vardan Khachatryan et al. Measurement of inclusive jet production and nuclear modifications in pPb collisions at $\sqrt{s_{NN}} = 5.02$ TeV. *Eur. Phys. J. C*, 76(7):372, 2016.
- [10] Shreyasi Acharya et al. Measurement of inclusive charged-particle b-jet production in pp and p-pb collisions at $\sqrt{s_{NN}} = 5.02$ tev. *JHEP*, 01:178, 2022.
- [11] Georges Aad et al. Strong Constraints on Jet Quenching in Centrality-Dependent p+Pb Collisions at 5.02 TeV from ATLAS. *Phys. Rev. Lett.*, 131(7):072301, 2023.
- [12] Shreyasi Acharya et al. Search for jet quenching effects in high-multiplicity pp collisions at $\sqrt{s} = 13$ TeV via di-jet acoplanarity. *JHEP*, 05:229, 2024.
- [13] B. Abelev and et al. Multiparticle azimuthal correlations in p -pb and pb-pb collisions at the cern large hadron collider. *Phys. Rev. C*, 90:054901, Nov 2014.
- [14] B. Abelev and et al. Elliptic flow of identified hadrons in Pb-Pb collisions at $\sqrt{s_{NN}} = 2.76$ TeV. *Journal of High Energy Physics*, 190:1029–8479, 2015.
- [15] Xiaoning Wang. Measurements of the azimuthal anisotropy of jets and high- p_T charged particles in Pb+Pb collisions with the ATLAS detector. *PoS, HardProbes2023*:159, 2024.
- [16] G. Agakishiev et al. Energy and system-size dependence of two- and four-particle v_2 measurements in heavy-ion collisions at RHIC and their implications on flow fluctuations and non-flow. *Phys. Rev. C*, 86:014904, 2012.
- [17] Vladimir Korotkikh. Elliptic flow studies in heavy-ion collisions using the CMS detector at the LHC. 12 2010.
- [18] A. M. Sirunyan and et al. Observation of correlated azimuthal anisotropy fourier harmonics in pp and $p + Pb$ collisions at the lhc. *Phys. Rev. Lett.*, 120:092301, Feb 2018.
- [19] V. Khachatryan and et al. Evidence for collective multiparticle correlations in p -Pb collisions. *Phys. Rev. Lett.*, 115:012301, Jun 2015.
- [20] Aleksi Kurkela, Urs Achim Wiedemann, and Bin Wu. Nearly isentropic flow at sizeable η/s . *Phys. Lett. B*, 783:274–279, 2018.
- [21] Victor E. Ambrus, S. Schlichting, and C. Werthmann. Development of transverse flow at small and large opacities in conformal kinetic theory. *Phys. Rev. D*, 105(1):014031, 2022.
- [22] Liang He, Terrence Edmonds, Zi-Wei Lin, Feng Liu, Denes Molnar, and Fuqiang Wang. Anisotropic parton escape is the dominant source of azimuthal anisotropy in transport models. *Phys. Lett. B*, 753:506–510, 2016.
- [23] Denes Molnar. How AMPT generates large elliptic flow with small cross sections. 6 2019.
- [24] Aleksi Kurkela, Aleksas Mazeliauskas, and Robin Törnkvist. Collective flow in single-hit QCD kinetic theory. *JHEP*, 11:216, 2021.
- [25] Ryan D. Weller and Paul Romatschke. One fluid to rule them all: viscous hydrodynamic description of event-by-event central p+p, p+Pb and Pb+Pb collisions at $\sqrt{s} = 5.02$ TeV. *Phys. Lett. B*, 774:351–356, 2017.
- [26] You Zhou, Wenbin Zhao, Koichi Murase, and Huichao Song. One fluid might not rule them all. *Nucl. Phys. A*, 1005:121908, 2021.
- [27] Georges Aad et al. Transverse momentum and process dependent azimuthal anisotropies in $\sqrt{s_{NN}} = 8.16$ TeV p +Pb collisions with the ATLAS detector. *Eur. Phys. J. C*, 80(1):73, 2020.
- [28] Shreyasi Acharya et al. Azimuthal anisotropy of jet particles in p-Pb and Pb-Pb collisions at $\sqrt{s_{NN}} = 5.02$ TeV. *JHEP*, 08:234, 2024.
- [29] Elliptic anisotropy at high p_T in pPb collisions using subevent cumulants. Technical report, CERN, Geneva, 2024.
- [30] Korinna C. Zapp, Frank Krauss, and Urs A. Wiedemann. A perturbative framework for jet quenching. *JHEP*, 1303:080, 2013.
- [31] Torbjorn Sjostrand, Stephen Mrenna, and Peter Skands. PYTHIA 6.4 physics and manual. *JHEP*, 05:026, 2006.
- [32] L. D. Landau and I. Pomeranchuk. Electron cascade process at very high-energies. *Dokl. Akad. Nauk Ser. Fiz.*, 92:735–738, 1953.
- [33] Arkady B. Migdal. Bremsstrahlung and pair production in condensed media at high-energies. *Phys. Rev.*, 103:1811–1820, 1956.
- [34] Korinna Christine Zapp, Johanna Stachel, and Urs Achim Wiedemann. A local Monte Carlo framework for coherent QCD parton energy loss. *JHEP*, 07:118, 2011.
- [35] Korinna C. Zapp. Geometrical aspects of jet quenching in JEWEL. *Phys. Lett. B*, 735:157–163, 2014.